On Tightening Aligned-Images Bounds Under Channel Uncertainty

Han Wu and Hamdi Joudeh
Information and Communication Theory Lab
Eindhoven University of Technology, The Netherlands
Email: {h.wu1, h.joudeh}@tue.nl

***Abstract*—We revisit the aligned-images approach put forth by Davoodi and Jafar in [1], and derive a tighter bound on the expected size of aligned image sets. This leads to an improved outer bound for a class of multiple-input deterministic broadcast channels with imperfect channel state information at the transmitter. The exact capacity remains unknown.**

I. Introduction

Aligned-images bounds were introduced in a seminal work by Davoodi and Jafar [1] to settle conjectures on the collapse of degrees-of-freedom (DoF) in the multiple-input single-output broadcast channel (MISO-BC) under finite precision channel state information at the transmitter (CSIT) [2], [3]. These bounds have since been further developed and extended to obtain tight DoF and generalized degrees-of-freedom (GDoF) outer bounds for various multiple-antenna and interference wireless networks under CSIT imperfections [4]–[13].

Aligned-images bounds are based on a combinatorial accounting of the maximum number of codewords that cast resolvable images at a desired receiver, while casting aligned images at an undesired receiver. While the roots of the aligned-images approach can be traced back to the work of Korner and Marton on images of sets via noisy channels [14], Davoodi and Jafar specialized and adapted the original idea to derive DoF and GDoF outer bounds for Gaussian networks with finite precision CSIT [1]. To facilitate the combinatorial argument in the aligned-images approach, a Gaussian channel model of interest is approximated by a deterministic (noiseless) counterpart with discrete inputs and outputs, see, e.g., [15]. The deterministic model de-emphasizes the role of noise, abstracted by the discrete input and output alphabets, and instead focuses on the interaction between signal strength and CSIT precision levels. Such a deterministic model maintains a capacity that is within a constant additive gap from its Gaussian counterpart's capacity, rendering it sufficient for obtaining tight DoF/GDoF characterizations (see the Appendix in [1]).

With optimal DoF and GDoF characterizations in hand, the natural next step is to pursue constant-gap capacity characterizations [16], with the ultimate goal of closing the gap to the exact capacity itself (see the discussion in [4, Sec. I.A]). Aligned-images bounds, at least in their current form, do not lead to obtaining constant-gap capacity characterizations. A prime example is the canonical 2-user MISO-BC setting under finite precision CSIT, considered in [1]. Here the gap between the best inner bound (i.e. achievable sum rate) and the aligned-images outer bound scales as $O(\log\log\sqrt{P})$, where P represents the transmitter power. While this gap is inconsequential for DoF/GDoF characterizations, it currently stands in the way of obtaining constant-gap capacity characterizations for wireless networks with finite precision CSIT.

In this paper, we make progress towards closing this gap through a simple refinement of the original aligned-images bound in [1] (see Section III). We focus on the deterministic 2-user MISO-BC setting of [1], described in detail in the following section, and we obtain a tighter outer bound for this channel. We conclude the paper with a conjecture on the capacity of this seemingly simple canonical setting.

II. Problem Setting and Preliminaries

Consider a 2-input, 2-output deterministic broadcast channel with the following input-output relationship

$$Y_1(t) = X_1(t) \tag{1}$$

$$Y_2(t) = \lfloor G(t)X_1(t)\rfloor + X_2(t) \tag{2}$$

where $t \in \mathbb{N}$ is the channel use index, $X_1(t), X_2(t) \in \mathbb{Z}$ are integer inputs, $Y_1(t), Y_2(t) \in \mathbb{Z}$ are integer outputs, and $G(t) \in \mathbb{R}$ is a real random channel state, and $\lfloor\cdot\rfloor$ denotes the floor function. $X_1(t)$ and $X_2(t)$ are restricted to the input alphabet $\mathcal{X} := [0 : A]$, where A is a positive integer. When considering n uses of this channel, we denote the input and output sequences as $\boldsymbol{X}_i := \big(X_i(1), \dots, X_i(n)\big)$ and $\boldsymbol{Y}_i := \big(Y_i(1), \dots, Y_i(n)\big)$, where $i \in \{1, 2\}$, and the channel state sequence as $\boldsymbol{G} := \big(G(1), \dots, G(n)\big)$. We therefore have

$$\boldsymbol{Y}_1 = \boldsymbol{X}_1 \text{ and } \boldsymbol{Y}_2 = \lfloor \boldsymbol{G} \circ \boldsymbol{X}_1\rfloor + \boldsymbol{X}_2. \tag{3}$$

where $\boldsymbol{G} \circ \boldsymbol{X}_1$ is an element-wise product.

One motivation for studying the above deterministic channel model is that it approximates the corresponding Gaussian broadcast channel with a 2-antenna transmitter, 2 single-antenna receivers, and a power constraint $P = O(A^2)$ [1].

A. Channel state uncertainty

We assume that the transmitter has an imperfect estimate of the channel state sequence $\boldsymbol{G}$. In particular, $\boldsymbol{G}$ is given by

$$\boldsymbol{G} = \hat{\boldsymbol{G}} + \tilde{\boldsymbol{G}} \tag{4}$$

where $\hat{\boldsymbol{G}} := \big(\hat{G}(1), \dots, \hat{G}(n)\big)$ and $\tilde{\boldsymbol{G}} := \big(\tilde{G}(1), \dots, \hat{G}(n)\big)$ model the transmitter's estimate and estimation error respectively, and $\hat{\boldsymbol{G}}$ and $\tilde{\boldsymbol{G}}$ are independent. We assume, without loss of generality, that the entries of $\tilde{\boldsymbol{G}}$ have zero mean.

The input $(\boldsymbol{X}_1, \boldsymbol{X}_2)$ may depend on the state estimate $\hat{\boldsymbol{G}}$, but is independent of $\tilde{\boldsymbol{G}}$, and hence the input distribution satisfies $P_{\boldsymbol{X}_1,\boldsymbol{X}_2|\boldsymbol{G},\hat{\boldsymbol{G}}}(\boldsymbol{x}_1,\boldsymbol{x}_2|\boldsymbol{g},\hat{\boldsymbol{g}}) = P_{\boldsymbol{X}_1,\boldsymbol{X}_2|\hat{\boldsymbol{G}}}(\boldsymbol{x}_1,\boldsymbol{x}_2|\hat{\boldsymbol{g}})$. We assume that receivers know $\boldsymbol{G}, \hat{\boldsymbol{G}}$ perfectly.

Bounded density assumption: For ease of exposition, we assume that the sequences $\boldsymbol{G}$ and $\hat{\boldsymbol{G}}$ are jointly i.i.d. with a joint distribution $f_{\boldsymbol{G},\hat{\boldsymbol{G}}}(\boldsymbol{g},\hat{\boldsymbol{g}}) = \prod_{t=1}^{n} f_{G,\hat{G}}(g(t),\hat{g}(t))$. Suppressing the index t, the pair $(G,\hat{G})$ satisfies the so-called bounded density assumption [1]. That is, the conditional probability density function of G given $\hat{G}$ is bounded above as

$$f_{G|\hat{G}}\big(g|\hat{g}\big) \leq f_{\max} \tag{5}$$

for some constant $f_{\max} < \infty$ (see also [4]–[7]). We assume, without loss of generality, that $f_{\max} \geq 1$. The bounded density assumption implies that from the transmitter's perspective, the channel state cannot be confined to a set of measure zero.

The maximum density value $f_{\max}$ is allowed to scale with A as $f_{\max} = A^{\alpha}$, where $\alpha \in [0,1]$ is a parameter that captures the quality of the channel state knowledge at the transmitter, i.e. CSIT quality parameter. Recall that A is proportional to $\sqrt{P}$, where P is a measure of power, or signal-to-noise ratio (SNR), in the corresponding Gaussian channel. The scaling $f_{\max} = A^{\alpha}$ allows for scenarios in which the precision of the channel estimate improves with SNR, and hence $f_{G|\hat{G}}\big(g|\hat{g}\big)$ becomes more concentrated. Such scaling is possible when there is, e.g., a feedback link of capacity $\alpha \log A$ from the receiver to the transmitter [17], [18].

B. Capacity

Consider the private message capacity of the above channel. We have independent messages W_1 and W_2 with rates R_1 and R_2, intended to receiver 1 and receiver 2, respectively. The capacity C is defined in the standard Shannon theoretic sense as the supremum of the sum rate $R_1 + R_2$.

The exact capacity C of this channel, under the channel state uncertainty model described above, is not known in general. However, lower and upper bounds are given as follows

$$C \geq (1+\alpha)\log A + O(1) \tag{6}$$

$$C \leq (1+\alpha)\log A + \log(1+\log A) + O(1) \tag{7}$$

where $O(1)$ is used to represent constant terms that do not depend on A, yet may depend on the choice of $f_{G,\hat{G}}(g,\hat{g})$. The lower bound in (6) can be inferred from achievability results for the counterpart Gaussian setting. Alternatively, we can obtain (6) by working directly with the deterministic channel model (see Remark 2 further on). The upper bound in (7) is obtained using the aligned-images approach [1].

The bounds in (6) and (7) lead to the following asymptotic characterization of the capacity pre-log factor:

$$d := \lim_{A\to\infty} \frac{C}{\log A} = 1 + \alpha \tag{8}$$

where d is also known as the DoF. The maximum admissible DoF in this settings is 2, achieved when $\alpha = 1$. For $\alpha = 0$, the DoF collapses to 1, and the channel behaves asymptotically like a single-input channel (e.g. single-antenna transmitter).

A more refined capacity characterization is one which is guaranteed to be within a constant gap from the capacity C for any choice of A. For such characterization, we need a lower bound C_{L} and an upper bound C_{U} that satisfy

$$C_{\mathrm{L}} \leq C_{\mathrm{U}} \leq C_{\mathrm{L}} + O(1). \tag{9}$$

Such characterization can be much more meaningful, especially when A is and not too large. The bounds in (6) and (7) are clearly not sufficient for obtaining a constant-gap capacity characterization due to the scaling gap of $O(\log\log A)$. In this paper, we make progress towards closing this gap.

C. Converse bound and aligned image sets

Using standard arguments, see, e.g. [1], one can write

$$nR_1 \leq I\big(W_1; \boldsymbol{Y}_1|W_2,\boldsymbol{G},\hat{\boldsymbol{G}}\big) + o(n) \tag{10}$$

$$= H(\boldsymbol{Y}_1|W_2,\boldsymbol{G},\hat{\boldsymbol{G}}) + o(n) \tag{11}$$

$$nR_2 \leq I\big(W_2; \boldsymbol{Y}_2|\boldsymbol{G},\hat{\boldsymbol{G}}\big) + o(n) \tag{12}$$

$$\leq n\log A - H(\boldsymbol{Y}_2|W_2,\boldsymbol{G},\hat{\boldsymbol{G}}) + nO(1) + o(n). \tag{13}$$

Therefore, finding an upper bound for the capacity boils down to bounding the following entropy difference:

$$H(\boldsymbol{Y}_1|W_2,\boldsymbol{G},\hat{\boldsymbol{G}}) - H(\boldsymbol{Y}_2|W_2,\boldsymbol{G},\hat{\boldsymbol{G}}) \tag{14}$$

Since $(\boldsymbol{X}_1,\boldsymbol{X}_2)$ may depend on $(W_2,\hat{\boldsymbol{G}})$, the entropy difference in (14) is maximized by optimizing the distribution $P_{\boldsymbol{X}_1,\boldsymbol{X}_2|W_2,\hat{\boldsymbol{G}}}(\boldsymbol{x}_1,\boldsymbol{x}_2|w_2,\hat{\boldsymbol{g}})$ for each realization $(w_2,\hat{\boldsymbol{g}})$. Therefore, we fix $(W_2,\hat{\boldsymbol{G}})$ to $(w_2,\hat{\boldsymbol{g}})$ henceforth, and suppress them from the conditioning for brevity. We now have an entropy difference $H(\boldsymbol{Y}_1|\boldsymbol{G}) - H(\boldsymbol{Y}_2|\boldsymbol{G})$, an input distribution $P_{\boldsymbol{X}_1,\boldsymbol{X}_2}(\boldsymbol{x}_1,\boldsymbol{x}_2)$, and a channel state $\boldsymbol{G} = \hat{\boldsymbol{g}} + \tilde{\boldsymbol{G}}$.

The upper bound in (7) is obtained by relating the entropy difference to the expected size of the corresponding aligned image set, as we see next. Assume that $\boldsymbol{X}_2 = \phi(\boldsymbol{X}_1)$, where $\phi : \mathcal{X}^n \to \mathcal{X}^n$ is some deterministic mapping. In this case we have $P_{\boldsymbol{X}_1,\boldsymbol{X}_2}(\boldsymbol{x}_1,\boldsymbol{x}_2) = P_{\boldsymbol{X}_1}(\boldsymbol{x}_1)\mathbb{1}\{\boldsymbol{x}_2 = \phi(\boldsymbol{x}_1)\}$, and the output $\boldsymbol{Y}_1$ is determined by the pair $(\boldsymbol{X}_1,\boldsymbol{G})$ as

$$\boldsymbol{Y}_2 = \lfloor \boldsymbol{G} \circ \boldsymbol{X}_1 \rfloor + \phi(\boldsymbol{X}_1). \tag{15}$$

Let $(\boldsymbol{x}_1,\boldsymbol{g})$ be a realization of $(\boldsymbol{X}_1,\boldsymbol{G})$. The corresponding aligned image set $\mathcal{S}_{\boldsymbol{x}_1}(\boldsymbol{g})$ is a subset of $\mathcal{X}^n$ defined as

$$\mathcal{S}_{\boldsymbol{x}_1}(\boldsymbol{g}) := \Big\{\boldsymbol{v} \in \mathcal{X}^n : \lfloor \boldsymbol{g} \circ \boldsymbol{v} \rfloor + \phi(\boldsymbol{v}) = \lfloor \boldsymbol{g} \circ \boldsymbol{x}_1 \rfloor + \phi(\boldsymbol{x}_1)\Big\}$$

that is the set of all inputs $\boldsymbol{X}_1$ that cast the same image in $\boldsymbol{Y}_2$. Since the pair $(\boldsymbol{X}_1,\boldsymbol{G})$ is random, the cardinality of the aligned image set $|\mathcal{S}_{\boldsymbol{X}_1}(\boldsymbol{G})|$ is a random variable. As shown in [1], the entropy difference is bounded above as

$$\max_{P_{\boldsymbol{X}_1,\boldsymbol{X}_2}} H(\boldsymbol{Y}_1|\boldsymbol{G}) - H(\boldsymbol{Y}_2|\boldsymbol{G}) \leq \max_{P_{\boldsymbol{X}_1},\phi} \mathbb{E}\log|\mathcal{S}_{\boldsymbol{X}_1}(\boldsymbol{G})| \tag{16}$$

$$\leq \max_{P_{\boldsymbol{X}_1},\phi} \log\mathbb{E}\,|\mathcal{S}_{\boldsymbol{X}_1}(\boldsymbol{G})| \tag{17}$$

where (17) is due to Jensen's inequality. Therefore, bounding the entropy difference reduces to bounding the expected size of the corresponding aligned image set. We conclude this section with the bound on $\mathbb{E}\,|\mathcal{S}_{\boldsymbol{X}_1}(\boldsymbol{G})|$ obtained in [1].

Theorem (Aligned-images [1]): The following bound holds

$$\frac{1}{n}\log\mathbb{E}\,|\mathcal{S}_{\boldsymbol{X}_1}(\boldsymbol{G})| \leq \log A^{\alpha} + \log(1+\log A) + O(1).$$

The above theorem yields the capacity upper bound in (7).

III. A Tighter Aligned-Images Bound

Here we present the main result of this paper, in which we tighten the upper bound in the previous theorem from [1].

Theorem 1: The following tightened bound holds

$$\frac{1}{n}\log\mathbb{E}\,|S_{\boldsymbol{X}_1}(\boldsymbol{G})| \leq \log A^{\alpha} + \log\bigl(1+\log A^{1-\alpha}\bigr) + O(1).$$

It follows directly from Theorem 1 and Section II-C that the capacity upper bound in (7) can be tightened to

$$C \leq (1+\alpha)\log A + \log\bigl(1+\log A^{1-\alpha}\bigr) + O(1). \tag{18}$$

A discussion of the new capacity upper bound in (18), as well as the upper bound in (7) and lower bound in (6), is presented in Section V. Next, we present a proof for Theorem 1.

A. Proof of Theorem 1 ($n = 1$)

It is quite instructive to start with the case $n = 1$. Given $X_1 = v$, the expected size of the aligned image set is

$$\begin{aligned}\mathbb{E}\,|\mathcal{S}_v(G)| &= \sum_{x_1\in\mathcal{X}}\mathbb{E}[\mathbb{1}\{x_1\in\mathcal{S}_v(G)\}]\\ &= \sum_{x_1=0}^{A}\mathbb{P}\{G : x_1\in\mathcal{S}_v(G)\} \qquad (19)\end{aligned}$$

where the above expectation is with respect to G. $\mathbb{P}\{G : x_1 \in S_v(G)\}$ is known as the probability of image alignment, i.e. the probability that inputs $(X_1, X_2) = (x_1, \phi(x_1))$ and $(X_1, X_2) = (v, \phi(v))$ cast the same image in Y_2. When $x_1 \neq v$, we have

$$\begin{aligned}&\mathbb{P}\{G : x_1\in\mathcal{S}_v(G)\}\\ &= \mathbb{P}\{G : \lfloor Gx_1\rfloor + \phi(x_1) = \lfloor Gv\rfloor + \phi(v)\} &(20)\\ &\leq \mathbb{P}\left\{G \in -\frac{\phi(x_1)-\phi(v)}{x_1-v} + \frac{\Delta_{(-1,1)}}{|x_1-v|}\right\} &(21)\end{aligned}$$

where $\Delta_{(-1,1)}$ denotes the interval $(-1, 1)$, and $c_1 + \frac{\Delta_{(-1,1)}}{c_2}$ denotes the interval $(c_1-\frac{1}{c_2}, c_1+\frac{1}{c_2})$, where $c_2 > 0$. Therefore, $\mathbb{P}\{G : x_1 \in S_v(G)\}$ is bounded above by the probability that G lies in an interval of length no more than $\frac{2}{|x_1-v|}$.

The key step to obtain the tightened bound is to partition the event $\{G : x_1 \in \mathcal{S}_v(G)\}$ with respect to some threshold on $\frac{2}{|x_1-v|}$. To this end, we define $\delta := \frac{1}{2}f_{\max}^{-1}$ and set the threshold as 2δ. This leads to a partition of $\{G : x_1 \in \mathcal{S}_v(G)\}$ with the following probability bounds

$$\mathbb{P}\left\{G : x_1\in\mathcal{S}_v(G), \frac{2}{|x_1-v|} < 2\delta\right\} \leq \frac{2}{|x_1-v|}f_{\max} \tag{22}$$

$$\mathbb{P}\left\{G : x_1\in\mathcal{S}_v(G), \frac{2}{|x_1-v|} \geq 2\delta\right\} \leq 1 = 2\delta f_{\max}. \tag{23}$$

Note (23) includes the case where $x_1 = v$, for which we have $\mathbb{P}\{G : x_1 \in \mathcal{S}_v(G), x_1 = v\} = 1$. It is also evident that

$$\frac{2}{|x_1-v|} < 2\delta \implies |x_1-v| > \left\lfloor\frac{1}{\delta}\right\rfloor \tag{24}$$

$$\frac{2}{|x_1-v|} \geq 2\delta \implies |x_1-v| \leq \left\lfloor\frac{1}{\delta}\right\rfloor \tag{25}$$

where the floor function in (25) follows from the fact that $|x_1 - v|$ must be an integer. Therefore, the probability of image alignment is bounded above as

$$\begin{aligned}\mathbb{P}\{G : x_1\in\mathcal{S}_v(G)\} \leq 2f_{\max}\Biggl(&\delta\mathbb{1}\left\{|x_1-v| \leq \left\lfloor\frac{1}{\delta}\right\rfloor\right\}+\\ &\frac{1}{|x_1-v|}\mathbb{1}\left\{|x_1-v| > \left\lfloor\frac{1}{\delta}\right\rfloor\right\}\Biggr).\end{aligned}$$

Plugging this upper bound back into (19), we obtain

$$\begin{aligned}&\mathbb{E}\,|\mathcal{S}_v(G)|\\ &\leq \sum_{x_1=0}^{A}\mathbb{P}\{G : x_1\in\mathcal{S}_v(G)\} &(26)\\ &\leq 2\sum_{|x_1-v|=0}^{A}\mathbb{P}\{G : x_1\in\mathcal{S}_v(G)\} &(27)\\ &\leq 4\sum_{|x_1-v|=0}^{A} f_{\max}\Biggl(\delta\mathbb{1}\left\{|x_1-v| \leq \left\lfloor\frac{1}{\delta}\right\rfloor\right\} +\\ &\qquad\qquad \frac{1}{|x_1-v|}\mathbb{1}\left\{|x_1-v| > \left\lfloor\frac{1}{\delta}\right\rfloor\right\}\Biggr) &(28)\\ &= 4f_{\max}\left(\underbrace{\delta+\delta+\cdots+\delta}_{\lfloor\frac{1}{\delta}\rfloor+1} + \frac{1}{\lceil\frac{1}{\delta}\rceil} + \cdots + \frac{1}{A}\right) &(29)\\ &\leq 4f_{\max}\Biggl(\ln(A) - \ln\left(\left\lfloor\frac{1}{\delta}\right\rfloor+1\right) +\\ &\qquad\qquad \delta\left\lfloor\frac{1}{\delta}\right\rfloor + \delta + 1\Biggr) &(30)\\ &\leq 4f_{\max}\left(\ln(A) - \ln\left(\left\lfloor\frac{1}{\delta}\right\rfloor+1\right) + 3\right) &(31)\\ &\leq 4f_{\max}\left(\ln(A) - \ln\left(\frac{1}{\delta}\right) + 3\right) &(32)\\ &= 4A^{\alpha}[(1-\alpha)\ln(A) + 3 - \ln 2]. &(33)\end{aligned}$$

In the above, (27) holds since the range of the summation in (26) is expanded from $0, 1, \cdots, A$ to $v-A, \cdots, v-1, v, v, v+1, \cdots, v+A$. (30) follows from the harmonic series

$$\ln(k+1) \leq \sum_{i=1}^{k}\frac{1}{i} \leq \ln(k) + 1.$$

(31) is a result of $\delta\lfloor\frac{1}{\delta}\rfloor + \delta + 1 \leq 1 + 1 + 1 = 3$, and (32) is due to $\lfloor x\rfloor + 1 > x$. The upper bound in (32) for $\mathbb{E}\,|\mathcal{S}_v(G)|$ holds for all $v \in \mathcal{X}$. Therefore, it follows that

$$\log\mathbb{E}\,|\mathcal{S}_{X_1}(G)| \leq \log A^{\alpha} + \log\bigl(1+\log A^{1-\alpha}\bigr) + O(1). \tag{34}$$

Remark 1: The above proof follows along the same footsteps of the original aligned-images proof in [1, Section. V]. The main additional step is the partitioning of the image alignment event in (22) and (23). Intuitively, the case in (22) includes outcomes of *weak* image alignment for which the probability of alignment is typically less than 1 and depends on the distance $|x_1 - v|$, i.e. a larger distance leads to a smaller alignment probability. On the other hand, (23) includes outcomes of *strong* image alignment, where the probability of alignment can be 1 (e.g. when $|x_1 - v|$ is small). In [1], the probability of image alignment is upper bounded by the bound in (22) for all values of $|x_1 - v|$. When $|x_1 - v|$ is small, (22) gives a loose overestimate of the probability of image alignment that may exceed 1. The tighter upper bound in (34) is obtained by introducing the event in (23), which bounds the probability of image alignment by 1 in strong alignment cases.

B. Proof of Theorem 1 ($n \geq 2$)

We extend the proof to the case when $n \geq 2$. We write

$$\mathbb{E}\,|\mathcal{S}_{\boldsymbol{v}}(G)| = \sum_{\boldsymbol{x}_1 \in \mathcal{X}^n} \mathbb{P}\{\boldsymbol{G} : \boldsymbol{x}_1 \in \mathcal{S}_{\boldsymbol{v}}(\boldsymbol{G})\}. \tag{35}$$

As in the case $n = 1$, whenever $\boldsymbol{x}_1 \neq \boldsymbol{v}$, the probability of image alignment is bounded above as

$$\begin{aligned}
&\mathbb{P}\{\boldsymbol{G} : \boldsymbol{x}_1 \in \mathcal{S}_{\boldsymbol{v}}(\boldsymbol{G})\} \\
&= \mathbb{P}\{\boldsymbol{G} : \lfloor \boldsymbol{G} \circ \boldsymbol{x}_1 \rfloor + \phi(\boldsymbol{x}_1) = \lfloor \boldsymbol{G} \circ \boldsymbol{v} \rfloor + \phi(\boldsymbol{v})\} && (36)\\
&\leq \prod_{t=1}^{n} \mathbb{P}\left\{ G(t) \in -\frac{\phi(x_1(t)) - \phi(v(t))}{x_1(t) - v(t)} + \frac{\Delta_{(-1,1)}}{|x_1(t) - v(t)|} \right\} && (37)\\
&\leq (2f_{\max})^n \prod_{t=1}^{n} \left[\delta \mathbb{1}\left\{ |x_1(t) - v(t)| \leq \left\lfloor \frac{1}{\delta} \right\rfloor \right\} + \right. \\
&\qquad \left. \frac{1}{|x_1(t) - v(t)|} \mathbb{1}\left\{ |x_1(t) - v(t)| > \left\lfloor \frac{1}{\delta} \right\rfloor \right\} \right]. && (38)
\end{aligned}$$

Note that the upper bound in (38) also holds whenever $\boldsymbol{x}_1 = \boldsymbol{v}$. Thus, it follows that

$$\begin{aligned}
&\mathbb{E}\,|\mathcal{S}_{\boldsymbol{v}}(\boldsymbol{G})| = \sum_{\boldsymbol{x}_1 \in \mathcal{X}^n} \mathbb{P}\{\boldsymbol{G} : \boldsymbol{x}_1 \in \mathcal{S}_{\boldsymbol{v}}(\boldsymbol{G})\} && (39)\\
&\leq \sum_{\boldsymbol{x}_1 \in \mathcal{X}^n} (2f_{\max})^n \prod_{t=1}^{n} \left[\delta \mathbb{1}\left\{ |x_1(t) - v(t)| \leq \left\lfloor \frac{1}{\delta} \right\rfloor \right\} + \right. \\
&\qquad \left. \frac{1}{|x_1(t) - v(t)|} \mathbb{1}\left\{ |x_1(t) - v(t)| > \left\lfloor \frac{1}{\delta} \right\rfloor \right\} \right] && (40)\\
&= (2f_{\max})^n \prod_{t=1}^{n} \left(\sum_{x_1(t)=0}^{A} \left[\delta \mathbb{1}\left\{ |x_1(t) - v(t)| \leq \left\lfloor \frac{1}{\delta} \right\rfloor \right\} + \right. \right. \\
&\qquad \left. \left. \frac{1}{|x_1(t) - v(t)|} \mathbb{1}\left\{ |x_1(t) - v(t)| > \left\lfloor \frac{1}{\delta} \right\rfloor \right\} \right] \right) && (41)\\
&\leq (4f_{\max})^n \prod_{t=1}^{n} \left(\sum_{|x_1(t)-v(t)|=0}^{A} \left[\delta \mathbb{1}\left\{ |x_1(t) - v(t)| \leq \left\lfloor \frac{1}{\delta} \right\rfloor \right\} \right. \right. \\
&\qquad \left. \left. + \frac{1}{|x_1(t) - v(t)|} \mathbb{1}\left\{ |x_1(t) - v(t)| > \left\lfloor \frac{1}{\delta} \right\rfloor \right\} \right] \right) && (42)\\
&\leq (4A^\alpha)^n [(1-\alpha)\ln(A) + 3 - \ln 2]^n && (43)
\end{aligned}$$

where (41) follows from the interchange of the sum and the product. Since this upper bound hold for all codeword realization $\boldsymbol{v} \in \mathcal{X}^n$, it follows that

$$\frac{1}{n} \log \mathbb{E}\,|S_{\boldsymbol{X}_1}(\boldsymbol{G})| \leq \log A^\alpha + \log\bigl(1 + \log A^{1-\alpha}\bigr) + O(1).$$

This completes the proof of Theorem 1.

IV. A Lower Bound on the Expected Size of Aligned Image Sets

Here we derive a simple lower bound for the expected size of aligned image sets in terms of the entropy difference in (16). For simplicity, we assume that $\hat{g} = 0$, and hence $G \sim f_G(g)$ has zero mean. We will show that the expected size of the aligned image set is bounded below as

$$\frac{1}{n} \max_{P_{\boldsymbol{X}_1}, \phi} \log \mathbb{E}\,|\mathcal{S}_{\boldsymbol{X}_1}(\boldsymbol{G})| \geq \log A^\alpha + O(1) \tag{44}$$

under common choices of the distribution $f_G(g)$. Therefore, after ignoring the $O(1)$ constant terms, there is an additive gap of $\log\bigl(1 + A^{1-\alpha}\bigr)$ between the lower bound in (44) and the new upper bound in Theorem 1.

To show (44), we choose $(\boldsymbol{X}_1, \boldsymbol{X}_2)$ such that $\boldsymbol{X}_2$ is fixed (e.g. all zeros), and $\boldsymbol{X}_1 \sim \prod_{t=1}^{n} P_{X_1}(x_1(t))$ is i.i.d. with each entry uniformly distributed on $[0 : \lfloor A^\alpha \rfloor]$ and has probability 0 elsewhere. Note that for such input, we have

$$H(\boldsymbol{Y}_1|\boldsymbol{G}) = nH(X_1) \geq n \log(A^\alpha) \tag{45}$$

as well as

$$\begin{aligned}
H(\boldsymbol{Y}_2|\boldsymbol{G}) &= nH(GX_1|G) && (46)\\
&\leq n\,\mathbb{E} \log\bigl(|G|(1 + A^\alpha)\bigr) && (47)\\
&\leq n \log(A^\alpha) + n + n \log(\mathbb{E}\,|G|). && (48)
\end{aligned}$$

From Section II-C, we know that the expected size of aligned image sets is bounded below in terms of the entropy difference. Combining this with (45) and (48), we have

$$\begin{aligned}
\max_{P_{\boldsymbol{X}_1}, \phi} \log \mathbb{E}\,|\mathcal{S}_{\boldsymbol{X}_1}(\boldsymbol{G})| &\geq H(\boldsymbol{Y}_1|\boldsymbol{G}) - H(\boldsymbol{Y}_2|\boldsymbol{G}) && (49)\\
&\geq -n\bigl(1 + \log(\mathbb{E}\,|G|)\bigr). && (50)
\end{aligned}$$

Next, we make some assumptions on the channel state distribution $f_G(g)$ to obtain the desired lower bound from (50).

1) Uniform G: Assume that $f_G(g)$ is a uniform distribution on the interval $[-\frac{A^{-\alpha}}{2}, \frac{A^{-\alpha}}{2}]$. Note that the interval is set so that $f_{\max} = A^\alpha$. Here we have $\mathbb{E}\,|G| = \frac{A^{-\alpha}}{4}$ and hence

$$H(\boldsymbol{Y}_1|\boldsymbol{G}) - H(\boldsymbol{Y}_2|\boldsymbol{G}) \geq \log A^\alpha + 1. \tag{51}$$

2) Gaussian G: Assume that $f_G(g)$ is a Gaussian distribution with zero mean and a standard deviation of $\sigma = \frac{A^{-\alpha}}{\sqrt{2\pi}}$. Note that here we also have $f_{\max} = A^\alpha$. In this case, $|G|$ has a half-normal distribution and $\mathbb{E}\,|G| = \sigma\sqrt{\frac{2}{\pi}} = \frac{A^{-\alpha}}{\pi}$. Therefore

$$H(\boldsymbol{Y}_1|\boldsymbol{G}) - H(\boldsymbol{Y}_2|\boldsymbol{G}) \geq \log A^\alpha + \log \pi - 1. \tag{52}$$

It is evident that in both of the above cases, the desired lower bound in (50) holds, albeit the constant term $O(1)$ may depend on the choice of distribution $f_G(g)$.

Remark 2: The above analysis can be used to prove the capacity lower bound in (6). In particular, we encode W_1 and W_2 into $\boldsymbol{X}_1$ and $\boldsymbol{X}_2$ respectively, i.e. $\boldsymbol{X}_1$ and $\boldsymbol{X}_2$ are chosen to be independent. Moreover, we choose $\boldsymbol{X}_1$ to be i.i.d. with entries uniform on $[0 : \lfloor A^\alpha \rfloor]$, while $\boldsymbol{X}_2$ is chosen to be i.i.d. with entries uniform on $[0 : A]$. We obtain:

$$\begin{aligned}
& I(\boldsymbol{X}_1; \boldsymbol{Y}_1|\boldsymbol{G}) + I(\boldsymbol{X}_2; \boldsymbol{Y}_2|\boldsymbol{G}) \\
& \quad = H(\boldsymbol{X}_1) + H(\boldsymbol{Y}_2|\boldsymbol{G}) - H(\boldsymbol{Y}_2|\boldsymbol{X}_2, \boldsymbol{G}) \\
& \quad \geq n \log A^\alpha + nO(1) + H(\boldsymbol{Y}_2|\boldsymbol{G}) && (53) \\
& \quad \geq n \log A^\alpha + nO(1) + H(\boldsymbol{Y}_2|\boldsymbol{X}_1, \boldsymbol{G}) && (54) \\
& \quad = n \log A^\alpha + nO(1) + H(\boldsymbol{X}_2) && (55) \\
& \quad \geq n \log A^\alpha + nO(1) + n \log A. && (56)
\end{aligned}$$

In (53), we used the fact that $H(\boldsymbol{X}_1) - H(\boldsymbol{Y}_2|\boldsymbol{X}_2, \boldsymbol{G})$ is equivalent to the entropy difference in (49), i.e.

$$\begin{aligned}
H(\boldsymbol{X}_1) - H(\boldsymbol{Y}_2|\boldsymbol{X}_2, \boldsymbol{G}) &= H(\boldsymbol{X}_1) - H(\lfloor \boldsymbol{G}\boldsymbol{X}_1 \rfloor | \boldsymbol{G}) \\
&\geq n \log A^\alpha + nO(1). \qquad (57)
\end{aligned}$$

In (54), we used the fact that conditioning does not increase entropy, and in (55) we used the independence of $\boldsymbol{X}_2$ and $(\boldsymbol{X}_1, \boldsymbol{G})$. Using standard channel coding arguments, the rates given by $R_1 = \frac{1}{n} I(\boldsymbol{X}_1; \boldsymbol{Y}_1|\boldsymbol{G})$ and $R_2 = \frac{1}{n} I(\boldsymbol{X}_2; \boldsymbol{Y}_2|\boldsymbol{G})$ are achievable, as $n \to \infty$. Hence, we have the capacity lower bound $C \geq \log A^{1+\alpha} + O(1)$.

V. Discussion

For illustration, the new capacity bound in (18), as well as the lower bound in (6) and the upper bound in (7), are shown in the figure below for $\alpha = 0.5$ and $\alpha = 0.9$. Note that we ignore the $O(1)$ constant terms for simplicity. As one would expect, the gap between the lower bound in (6) and new upper bound in (18) gets smaller as α increases. The tightness of the new upper bound is explored further below.

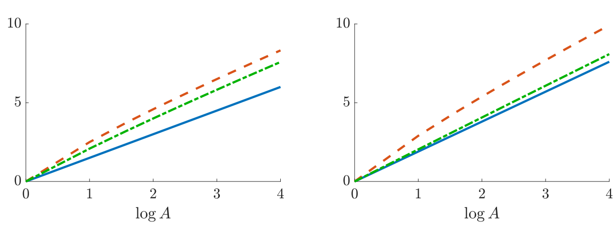

Fig. 1. Capacity bounds without the constants. Left: $\alpha = 0.5$. Right: $\alpha = 0.9$. Blue solid line: $\log A^{1+\alpha}$ (lower bound). Red dashed line: $\log A^{1+\alpha} + \log(1 + \log A)$ (upper bound in [1]). Green dash-dot line: $\log A^{1+\alpha} + \log\big(1 + \log A^{1-\alpha}\big)$ (tightened upper bound in Theorem 1).

In addition to the upper bounds (7) and (18), a trivial upper bound for the capacity is given by

$$C \leq 2 \log A + O(1). \qquad (58)$$

This upper bound is obtained by allowing the two receivers to fully cooperative, hence reducing the broadcast channel to a point-to-point channel with 2-inputs and 2-outputs. In particular, continuing from (10) and (12) while dropping the $o(n)$ term, the upper bound in (58) is obtained as

$$\begin{aligned}
n(R_1 + R_2) &\leq I\big(W_1; \boldsymbol{Y}_1|W_2, \boldsymbol{G}\big) + I\big(W_2; \boldsymbol{Y}_2|\boldsymbol{G}\big) \\
&\leq I\big(W_1; \boldsymbol{Y}_1, \boldsymbol{Y}_2|W_2, \boldsymbol{G}\big) + I\big(W_2; \boldsymbol{Y}_1, \boldsymbol{Y}_2|\boldsymbol{G}\big) \\
&= I(\boldsymbol{X}_1, \boldsymbol{X}_2; \boldsymbol{Y}_1, \boldsymbol{Y}_2|\boldsymbol{G}) \\
&= H(\boldsymbol{Y}_1, \boldsymbol{Y}_2|\boldsymbol{G}) \\
&= H(\boldsymbol{Y}_1|\boldsymbol{G}) + H(\boldsymbol{Y}_2|\boldsymbol{Y}_1, \boldsymbol{G}) \\
&= H(\boldsymbol{X}_1) + H(\boldsymbol{Y}_2|\boldsymbol{X}_1, \boldsymbol{G}) \\
&= H(\boldsymbol{X}_1) + H(\boldsymbol{X}_2) \\
&\leq 2n \log(1 + A). \qquad (59)
\end{aligned}$$

Note that (58) does not depend on α, which is expected as it is well known that the point-to-point multiple-input multiple-output (MIMO) channel is *robust* against CSIT imperfections.

The cooperative upper bound in (58) is achievable (up to a constant additive gap) in the broadcast channel when $\alpha = 1$, which follows by observing that (58) matches the lower bound in (56) in this case. Interestingly, our new capacity upper bound in (18) also matches the cooperative upper bound in (58) when $\alpha = 1$. On the other hand, the capacity upper bound of [1] given in (7) is always loose, even when $\alpha = 1$.

For the more interesting case of $\alpha < 1$, the capacity remains an open problem, and even a constant-gap characterization of the capacity is not yet known. With the improved upper bound in (18), the current standing is as follows:

$$\begin{aligned}
& C \geq \log A^{1+\alpha} + O(1) && (60) \\
& C \leq \log A^{1+\alpha} + \log\big(1 + \log A^{1-\alpha}\big) + O(1). && (61)
\end{aligned}$$

Nevertheless, it is not year clear which of the above bounds is tight. We conjecture that the upper bound is loose.

Conjecture: We conjecture that the lower bound in (60) is tight, up to a constant gap. That is, the capacity of the deterministic broadcast channel described in Section II is

$$C = (1 + \alpha) \log A + O(1) \qquad (62)$$

where $O(1)$ is a constant that does not depend on A.

Recall that to find an upper bound for the capacity, we bound the entropy difference $H(\boldsymbol{Y}_1|\boldsymbol{G}) - H(\boldsymbol{Y}_2|\boldsymbol{G})$, which in turn is bounded above by the expected logarithm of the size of the aligned image set, i.e. $\mathbb{E} \log |\mathcal{S}_{\boldsymbol{X}_1}(\boldsymbol{G})|$, as seen in (16). The term $\mathbb{E} \log |\mathcal{S}_{\boldsymbol{X}_1}(\boldsymbol{G})|$ is further bounded above by $\log \mathbb{E} |\mathcal{S}_{\boldsymbol{X}_1}(\boldsymbol{G})|$ using Jensen's inequality. This reduces the problem to bounding the expected size of the aligned image set, which is accomplished by bounding the probabilities of image alignment as seen in Section III-A. It is plausible that the application of Jensen's inequality and the bounding of $\log \mathbb{E} |\mathcal{S}_{\boldsymbol{X}_1}(\boldsymbol{G})|$ are the causes of looseness. To get a tighter upper bound on the entropy difference, one may have to work directly with $\mathbb{E} \log |\mathcal{S}_{\boldsymbol{X}_1}(\boldsymbol{G})|$ instead of $\log \mathbb{E} |\mathcal{S}_{\boldsymbol{X}_1}(\boldsymbol{G})|$, which may lead to resolving the above conjecture.

REFERENCES

[1] A. G. Davoodi and S. A. Jafar, "Aligned image sets under channel uncertainty: Settling conjectures on the collapse of degrees of freedom under finite precision CSIT," *IEEE Trans. Inf. Theory*, vol. 62, no. 10, pp. 5603–5618, 2016.

[2] A. Lapidoth, S. Shamai, and M. Wigger, "On the capacity of fading MIMO broadcast channels with imperfect transmitter side-information," in *Proc. 43rd Annu. Allerton Conf. Commun., Control Comput.*, 2005.

[3] R. Tandon, S. A. Jafar, S. Shamai, and H. V. Poor, "On the synergistic benefits of alternating CSIT for the MISO broadcast channel," *IEEE Trans. Inf. Theory*, vol. 59, no. 7, pp. 4106–4128, 2013.

[4] A. G. Davoodi and S. A. Jafar, "Transmitter cooperation under finite precision CSIT: A GDoF perspective," *IEEE Trans. Inf. Theory*, vol. 63, no. 9, pp. 6020–6030, 2017.

[5] ——, "Generalized degrees of freedom of the symmetric K user interference channel under finite precision CSIT," *IEEE Trans. Inf. Theory*, vol. 63, no. 10, pp. 6561–6572, 2017.

[6] A. G. Davoodi, B. Yuan, and S. A. Jafar, "GDoF region of the MISO BC: Bridging the gap between finite precision and perfect CSIT," *IEEE Trans. Inf. Theory*, vol. 64, no. 11, pp. 7208–7217, 2018.

[7] A. G. Davoodi and S. A. Jafar, "Optimality of simple layered superposition coding in the 3 user MISO BC with finite precision CSIT," *IEEE Trans. Inf. Theory*, vol. 65, no. 11, pp. 7181–7207, 2019.

[8] ——, "Degrees of freedom region of the (M, N_1, N_2) MIMO broadcast channel with partial CSIT: An application of sum-set inequalities based on aligned image sets," *IEEE Trans. Inf. Theory*, vol. 66, no. 10, pp. 6256–6279, 2020.

[9] ——, "Sum-set inequalities from aligned image sets: Instruments for robust GDoF bounds," *IEEE Trans. Inf. Theory*, vol. 66, no. 10, pp. 6458–6487, 2020.

[10] H. Joudeh and B. Clerckx, "On the separability of parallel MISO broadcast channels under partial CSIT: A degrees of freedom region perspective," *IEEE Trans. Inf. Theory*, vol. 66, no. 7, pp. 4513–4529, 2020.

[11] J. Wang, B. Yuan, L. Huang, and S. A. Jafar, "Sum-GDoF of 2-user interference channel with limited cooperation under finite precision CSIT," *IEEE Trans. Inf. Theory*, vol. 66, no. 11, pp. 6999–7021, 2020.

[12] Y. Chan, J. Wang, and S. A. Jafar, "Toward an extremal network theory—robust GDoF gain of transmitter cooperation over TIN," *IEEE Trans. Inf. Theory*, vol. 66, no. 6, pp. 3827–3845, 2020.

[13] H. Joudeh and G. Caire, "Cellular networks with finite precision CSIT: GDoF optimality of multi-cell TIN and extremal gains of multi-cell cooperation," *arXiv:2008.08945*, 2020.

[14] J. Korner and K. Marton, "Images of a set via two channels and their role in multi-user communication," *IEEE Trans. Inf. Theory*, vol. 23, no. 6, pp. 751–761, 1977.

[15] A. S. Avestimehr, S. N. Diggavi, C. Tian, and D. N. C. Tse, "An approximation approach to network information theory," *Found. Trends Commun. Inf. Theory*, vol. 12, no. 1-2, pp. 1–183, 2015.

[16] R. H. Etkin, D. N. C. Tse, and H. Wang, "Gaussian interference channel capacity to within one bit," *IEEE Trans. Inf. Theory*, vol. 54, no. 12, pp. 5534–5562, 2008.

[17] N. Jindal, "MIMO broadcast channels with finite-rate feedback," *IEEE Trans. Inf. Theory*, vol. 52, no. 11, pp. 5045–5060, 2006.

[18] G. Caire, N. Jindal, M. Kobayashi, and N. Ravindran, "Multiuser MIMO achievable rates with downlink training and channel state feedback," *IEEE Trans. Inf. Theory*, vol. 56, no. 6, pp. 2845–2866, 2010.